

Inverse modelling for estimating sorption and degradation parameters for pesticides

Igor G Dubus,^{1*} Sabine Beulke,¹ Colin D Brown,¹ Bernhard Gottesbüren² and Angelika Dienes²

¹Cranfield Centre for EcoChemistry, Cranfield University, Silsoe, Bedfordshire, MK45 4DT, UK

²BASF AG, Crop Protection Division, PO Box 120, 67114 Limburgerhof, Germany

Abstract: The leaching model PESTRAS was used to estimate sorption and degradation values for bentazone from three lysimeter datasets using the inverse modelling package PEST. Investigations were undertaken to assess the influence on calibration results of (1) values attributed to uncertain parameters not included in the calibration, and (2) starting values supplied to the inverse modelling package. Automatic calibrations with different realistic values for the Freundlich exponent n_f yielded different combinations of K_{om} and DT_{50} . Similarly, the supply of different starting values for K_{om} and DT_{50} revealed that different combinations of these two parameters equally calibrated PESTRAS for two of the three lysimeters. Examination of the error surface, ie the forward running of the model for different combinations of K_{om} and DT_{50} values, and the calculation of the goodness-of-fit to the experimental data, was found useful for identifying those instances where non-uniqueness in the calibration is likely to occur. Although the derivation of sorption and degradation values through inverse modelling is expected to offer significant benefits over laboratory determinations, care should be exercised when examining values derived through this approach. Research is needed to identify data requirements for robust estimation of sorption and degradation parameters through calibration of pesticide fate models against leaching data.

© 2004 Society of Chemical Industry

Keywords: inverse modelling; calibration; parameter estimation; response surface analysis

1 INTRODUCTION

Mathematical modelling has increasingly been used in the last two decades to describe and predict the fate of agrochemicals in the environment, particularly the transfer of compounds to surface waters and groundwater. Compared with standard field studies, the use of pesticide fate models is cost- and time-effective and does not rely on rainfall and other environmental factors to yield results of interest. Furthermore, it offers the possibility of encompassing the variability of weather conditions through the use of long-term data series, and offers some extrapolation capabilities to other climates, soils and cropping practices. As a result of the numerous benefits of modelling, a large number of models have been developed, contrasting in their complexity, parameter requirements and their intended use. Given the complex nature of processes involved in the transfer of pesticides in soil, calibration activities are often at the heart of any modelling activity in this field.¹

Automatic calibration of a model against experimental data by varying model parameters has been used extensively in groundwater hydrological modelling,² soil water physics³ and surface water hydrology,⁴ and

is referred to as inverse modelling. Universal inverse modelling packages such as PEST⁵ or UCODE⁶ can be linked to almost any model provided it uses and produces ASCII files and can be run in batch mode. The large majority of pesticide leaching models meet these criteria. The application of inverse modelling methods to pesticide fate models is expected to have numerous advantages. Three specific uses can be anticipated. First, inverse modelling provides a means to automatically calibrate models against experimental data, and is therefore a welcome alternative to time-consuming and subjective trial-and-error methods that are currently used in the calibration of water and pesticide components of pesticide leaching models. Although the tuning of some parameters manually until the model matches the data in some—often vague and subjective—sense can be rather successful in applications where the number of parameters is small, it suffers from a lack of exactness, reproducibility and objectivity.⁷ Second, inverse modelling techniques could help determine adequate values for the most uncertain model input parameters that cannot be determined routinely through experimentation or expert judgement.⁸ The third use, investigated here,

* Correspondence to: Igor G Dubus, BRGM, Avenue C. Guillemin, BP 6009, 45060 Orléans Cedex 2, France

E-mail: i.dubus@brgm.fr

Contract/grant sponsor: BASF AG

(Received 6 January 2004; revised version received 9 February 2004; accepted 23 February 2004)

Published online 27 April 2004

envisages that inverse modelling may be used to derive sorption and degradation parameters that are specific to field conditions.

Sorption and degradation parameters usually have the largest influence on predictions for leached load or maximum concentrations in leachate from pesticide leaching models.^{9–11} Since sorption and degradation processes cannot be measured independently in the field, the parameters required are traditionally determined in laboratory experiments under controlled conditions. However, there are doubts in some instances on the use of laboratory values to describe pesticide fate under outdoor conditions.^{12,13} Innovative laboratory methods that attempt to reproduce field conditions more closely have been investigated,¹⁴ but no method has gained widespread acceptance, and sorption and degradation parameters derived under controlled laboratory conditions remain the norm. An alternative which may appear promising is the use of data collected during field or lysimeter experiments to determine those parameters. This can be achieved through calibration of a pesticide leaching model for sorption and degradation parameters against experimental fate data acquired under outdoor conditions.

An evaluation of the combination of the inverse modelling package PEST with the leaching model PESTRAS (PESticide TRansport ASsessment) has been undertaken. The present paper reports on the simulation of leaching of bentazone from three lysimeters, and on the possibility of deriving sorption and degradation parameters from lysimeter data through an inverse modelling approach. Issues of reliability in the derivation of sorption and degradation parameters were investigated by assessing the influence on calibration results of (1) values attributed to uncertain parameters not included in the calibration, and (2) starting values supplied to the inverse

modelling package. A response surface analysis was also undertaken to assess the confidence that should be attributed to calibration results.

2 MATERIALS AND METHODS

2.1 Soils and lysimeter experiments

As part of the regulatory submission for the contact herbicide bentazone, three lysimeter experiments using sandy loam soils were conducted in Germany following BBA guidelines.¹⁵ Selected physico-chemical and hydrological properties are presented in Table 1 for the three soils used. The lysimeters, which ranged from 1 to 1.2 m in depth, were cropped and managed according to good agricultural practice (Table 2). The surface area was 1 m². ¹⁴C-Bentazone was applied to all lysimeters as a water-soluble formulation between the end of March and the beginning of July at application rates ranging from 0.9 to 1.35 kg AI ha⁻¹. A single application (in the first year) was made to lysimeters 1 and 3 while bentazone was applied twice to lysimeter 2 (one application in the first year, one application in the second year). Lysimeters 1 and 2 had to be irrigated to meet the German BBA guideline for lysimeter studies (annual rainfall >800 mm). Leachate from the lysimeters was sampled at regular intervals and analysed for total radioactivity by liquid scintillation counting and for concentrations of the herbicide by thin layer chromatography and/or GC-MS. Concentrations presented are those determined by these latter two methods.

2.2 PESTRAS modelling

The PESTRAS model¹⁶ was used in its version 3.1.3 to simulate water and herbicide movement through the lysimeters using site-specific weather data. PESTRAS

Table 1. Selected physico-chemical properties for the three soils and Van Genuchten parameters used in the modelling

Depth (cm)	Physico-chemical properties				Parameters of the Van Genuchten equation			
	Sand (%)	Silt (%)	Clay (%)	OM (%)	θ_s (m ³ m ⁻³)	θ_r (m ³ m ⁻³)	α (m ⁻¹)	n
Borstel soil								
0–30	68.3	24.5	7.2	2.6	0.391	0.030	1.26	1.47
30–57	67.0	26.3	6.7	1.7	0.370	0.029	1.81	1.57
57–73	96.2	2.9	0.9	0.3	0.351	0.015	2.81	1.60
73–90	99.8	0.2	0.0	0.0	0.310	0.015	2.81	1.61
90–110	100.0	0.0	0.0	0.0	0.310	0.015	2.81	1.61
110–120	100.0	0.0	0.0	0.0	0.310	0.015	2.81	1.61
Schifferstadt soil								
0–35	75.8	16.5	7.7	1.5	0.430	0.020	2.27	1.55
35–60	76.3	14.0	9.7	0.7	0.360	0.010	2.24	2.17
60–80	87.5	5.2	7.3	0.2	0.360	0.010	2.24	2.17
80–110	90.1	6.3	3.6	0.3	0.360	0.010	2.24	2.17
110–120	90.1	6.3	3.6	0.3	0.360	0.010	2.24	2.17
Landau soil								
0–39	54.0	39.0	7.0	2.7	0.430	0.020	2.27	1.55
39–85	47.0	44.0	9.0	0.8	0.460	0.000	0.94	1.44
85–90	92.0	0.0	8.0	0.6	0.360	0.010	2.24	2.17
90–100	92.0	0.0	8.0	0.6	0.360	0.010	2.24	2.17

Table 2. Selected characteristics of the three lysimeter studies

Lysimeter number	Location ^a	Soil name	Cropping ^b	Duration (years)	Total water input ^c (mm)	Sampling points
1	A	Borstel	Cereals	2	1620	15
2	A	Schifferstadt	WC–WO	3	2414	19
3	B	Landau	Vegetables–WC	3	2813	42

^a A: Limburgerhof; B: Schmallenberg.

^b WC: winter cereals; WO: winter oilseed rape.

^c Rainfall + irrigation.

is a one-dimensional multi-layer model that includes sub-routines on water and solute transport, sorption, transformation, volatilisation and plant uptake of solutes. Water and solute transport are based on the Richards' and convection–dispersion equations, respectively. Pesticide degradation is assumed to follow first-order kinetics and sorption is considered to be instantaneously at equilibrium and to be described by a Freundlich isotherm. The PESTRAS model has been evaluated against data for a sandy soil at Vredepeel in The Netherlands and showed good capabilities in predicting the leaching of bromide and two herbicides in the field when site-specific parameter values were used.¹⁷

For the present exercise, hydrological parameters required by PESTRAS were obtained by fitting the van Genuchten equation¹⁸ where measured water release curves were available. Alternatively, data were obtained from those given for eight textural classes by Tiktak *et al.*¹⁹ using data for the Dutch 'Winand Staring soil series' and the Dutch 'old soil series' (Table 1). The soil classes were selected on the basis of the measured clay, silt and organic matter contents.

PESTRAS does not include an explicit lysimeter bottom boundary condition. Following suggestions from the model author, the bottom boundary was set to 'free drain' and the parameter α of the van Genuchten equation was arbitrarily fixed to 100 times the value estimated for the soils within the bottom 10 cm of the profile. This bottom thickness was arbitrarily selected. With these settings, outflow only occurs when the bottom layer is virtually saturated, and thus reflects the specific conditions in zero-suction lysimeters.

The crops grown in the three lysimeters are listed in Table 2. The time-course of leaf area indices for cereals was taken from Dikau²⁰ and Knisel²¹ and adapted to the actual sowing and harvest dates. Leaf area indices given by Hough²² were used as a basis for simulating winter oilseed rape and vegetables, and crop growth stages were used to derive the interception of the application solution by the crops. Since some soils were cultivated to *ca* 20 cm depth at the end of each vegetation period or shortly before sowing the subsequent crop, the ploughing option of PESTRAS was used. This enabled uniform redistribution of pesticide residues in the plough layer at the end of each season. Crop parameters that influence evapotranspiration were calibrated manually within reasonable limits ('trial-and-error calibration')

to achieve a good agreement between measured and observed volumes of leachate.

Equilibrium sorption in PESTRAS is simulated using the Freundlich equation:

$$X = K_f \times C_e^{n_f} \quad (1)$$

where X is the amount of compound sorbed (kg kg^{-1}), K_f is the Freundlich sorption distribution coefficient ($\text{m}^{3/n} \text{kg}^{-1/n}$), C_e is the concentration of the compound in solution at equilibrium (kg m^{-3}) and n_f is the Freundlich exponent.

In PESTRAS, K_f is estimated from the Freundlich sorption distribution coefficient normalised to organic matter (K_{om}) using the following equation:

$$K_f = f_{om} \times K_{om} * C_r^{1-n_f} \quad (2)$$

where f_{om} is the mass fraction of soil organic matter (kg kg^{-1}) and C_r is the concentration at which the equilibrium concentration has been estimated (reference concentration; kg m^{-3}).

No data specific to the lysimeters on sorption and degradation of bentazone were available. Sorption (the sorption distribution coefficient normalised to organic matter K_{om} and the Freundlich exponent n_f) and degradation (the time for 50% of the pesticide to degrade in an incubation experiment as derived by first-order kinetics, DT_{50}) parameters were set to median values as calculated from 11 sorption and 21 degradation experiments (Table 3; Company data). The half-life used ($DT_{50} = 17.8$ days at 20°C) was larger than the median of 10 field persistence studies ($DT_{50} = 12.5$ days). These median estimates for K_{om} and DT_{50} were used as starting values for the inverse modelling. Degradation rates in the subsoil

Table 3. Sorption and degradation data for bentazone (unpublished data)

	Sorption		Degradation	
	K_{om} (ml g^{-1})	n_f	Laboratory half-life (days)	Field DT_{50} (days)
Number of studies	11	11	21	10
Minimum	3.7	0.561	7.1	3.0
Maximum	101.9	1.125	86.6	21.0
Mean	26.1	0.839	25.9	12.9
Median	16.4	0.800	17.8	12.5

were calculated from those in the topsoil in proportion to the organic matter content of the various horizons. Henry's constant was set to zero, as no significant loss of bentazone through volatilisation has been reported previously.

2.3 Inverse modelling

Inverse modelling was carried out using the parameter estimation package PEST⁵ which implements a modified version of the Gauss–Marquardt–Levenberg non-linear estimation algorithm. PEST controls a model by communicating with it through its input and output files, and will adjust selected input parameters as it runs the model repeatedly until the fit between selected output from the model and experimental data is optimised according to the weighted least squares criterion. The range of variation of parameters can be specified to avoid the return of unreasonable estimates by PEST. Since the package dialogues with model input and output files only, it can be used with virtually any command-line-driven model without the need for recoding and thus has wide applicability.

The inverse modelling exercise was limited to the calibration of K_{om} and DT_{50} which are two of the most sensitive input parameters for the PESTRAS model.¹⁶ The Freundlich exponent n_f was not included in the calibrations since K_{om} and n_f can be expected to compensate for one another in the modelling to some extent. Variations of K_{om} and DT_{50} were restricted to positive values by allowing the parameters to vary between 10^{-10} and 10^{10} . Target experimental values for model optimisation were bentazone concentrations in samples taken from each of the three lysimeters. Lysimeter experiments to investigate the fate of pesticides provide a number of sampling points during the year with varying time intervals between them. Each sample is therefore an integration of pesticide leached through the soil core during the interval between two successive sampling occasions. Since PESTRAS does not offer the possibility of calculating pesticide concentrations integrated over time periods, a program was written in Perl²³ to compute them. Output from the Perl program was compared with experimental data by PEST at each model run to assess the goodness of fit. All sampling points were included in the dataset, and concentrations below the analytical limit of quantification ($0.01 \mu\text{g litre}^{-1}$) were set to half that value. Default values related to termination criteria and calculation of derivatives supplied by PEST were used. The same weights were assigned to all observations.

The research on the capability of inverse modelling to provide robust estimates of K_{om} and DT_{50} involved four phases. In a first step, a unique combination of starting values was attributed to K_{om} and DT_{50} (median value from 11 sorption experiments for K_{om} , median value from 21 degradation experiments for DT_{50}) and these parameters were optimised by inverse modelling for the three lysimeters. In the second and third steps, investigations were undertaken on

the influence on optimised parameters of (1) the attribution of different values to the Freundlich exponent n_f ; and, (2) the use of various combinations of starting values for K_{om} and DT_{50} . Finally, a response surface analysis which involves running PESTRAS in a forward manner with a range of K_{om} and DT_{50} values was undertaken.

2.4 Influence of n_f values on calibration results

Estimates of K_{om} and n_f values used in the initial calibration exercises (K_{om} 16.4 ml g^{-1} ; n_f 0.8) were taken as the median of 11 values obtained in batch equilibrium sorption experiments. Here, the influence of the n_f value on calibration results was investigated to address the uncertainty in the attribution of a value to this parameter. Calibrations similar to those described above were conducted for different n_f values. These were varied between 0.56 and 1.12 (the minimum and maximum values reported in laboratory experiments) using a 0.01-unit increment. This resulted in 57 calibration exercises for each of the three lysimeters. At the end of each calibration, optimised values, correlation between K_{om} and DT_{50} , the number of runs to achieve convergence, eigenvalues and the value for the objective function were stored for later analysis.

2.5 Influence of starting values on calibration results

A single combination of starting values was used in the initial calibrations for the three lysimeters (K_{om} 16.4 ml g^{-1} ; DT_{50} 17.8 days). Here, the influence on calibration results of starting values provided to the PEST package⁵ was investigated for the three datasets selected. Combinations of starting values for K_{om} and DT_{50} were obtained by varying K_{om} between 2 and 30 ml g^{-1} and DT_{50} between 2 and 30 days using an increment of 2 units for each parameter and by combining all possible K_{om} and DT_{50} values. This resulted in a total of 225 calibration exercises for each of the three datasets. For each calibration performed, the following information was extracted from the PEST record file: values for K_{om} and DT_{50} at the end of the calibration, number of model runs carried out, reason for ending the calibration, sum of squared residuals and correlation between K_{om} and DT_{50} within the calibration.

2.6 Response surface analysis

The PESTRAS model was run in a forward manner (as opposed to the inverse modelling approach) for multiple combinations of K_{om} and DT_{50} values. Parameter values were varied between 2 and 30 ml g^{-1} (40 ml g^{-1} for lysimeter 3) and between 2 and 30 days (40 days for lysimeter 3) for K_{om} and DT_{50} , respectively. An increment of one unit was applied to both parameters and this resulted in a total of 841 combinations (1521 combinations for lysimeter 3) of K_{om} and DT_{50} . A model run was performed for each of these combinations and the sum of squared residuals

(Φ statistics) which is used by PEST for assessing the lack-of-fit was calculated for each run:

$$\Phi = \sum_{i=1}^n \omega_i^2 \times (O_i - P_i)^2$$

where O_i is the i th observed concentration, P_i is the model prediction for the i th concentration, ω_i is the weight attributed to the i th observation (here $\omega_i = 1$ for all observations) and n is the number of observations.

The lack- (Φ) and goodness- (Φ^{-1}) of-fit was analysed using a three-dimensional (3D) representation against K_{om} and DT_{50} values. As noted by Hopmans and Šimunek,³ response surface analysis is helpful in revealing the occurrence of local minima, the presence of a well-defined global minimum, parameter sensitivity and correlation. The technique has recently been used by Roulier and Jarvis^{8,24} in an effort to investigate parameter correlation in calibration activities undertaken with the pesticide leaching model MACRO.

3 RESULTS

3.1 Water balance trial-and-error calibration and herbicide leaching prior to automatic calibration of K_{om} and DT_{50}

Figure 1 presents a comparison of measured cumulative volumes of lysimeter leachates and those simulated after calibration of PESTRAS by varying crop parameters manually in an iterative process. Overall, a good agreement between observed and simulated water balances was achieved. Although actual volumes of water collected from lysimeter 3 were relatively well matched by the model before day 390 and from day 461 onwards, an over-estimation between these two dates resulted in a large over-estimation of cumulative leachate. It was not possible to achieve a better fit by calibrating crop parameters alone.

Leaching of bentazone for the three lysimeters was first predicted by PESTRAS using the median values for K_{om} , n_f and DT_{50} calculated from laboratory data. Figure 2 presents the observed concentrations in leachate and integrated concentrations as calculated from PESTRAS daily output. Maximum concentrations and cumulative loads over the experimental periods are presented in Table 4. The observed maximum concentration and cumulative loads leached through lysimeter 1 were well represented by the model prior to calibration of pesticide parameters (Table 4). However, the simulated timings of first breakthrough and of peak concentrations did not match those observed (Fig 2). In addition, the large concentration appearing at the end of the sampling period was not simulated by the model. PESTRAS was not able to predict leaching of the herbicide through the Schifferstadt soil (lysimeter 2) on the basis of the starting K_{om} and DT_{50} values used. Large discrepancies were observed for the lysimeter, although this may be attributed to some

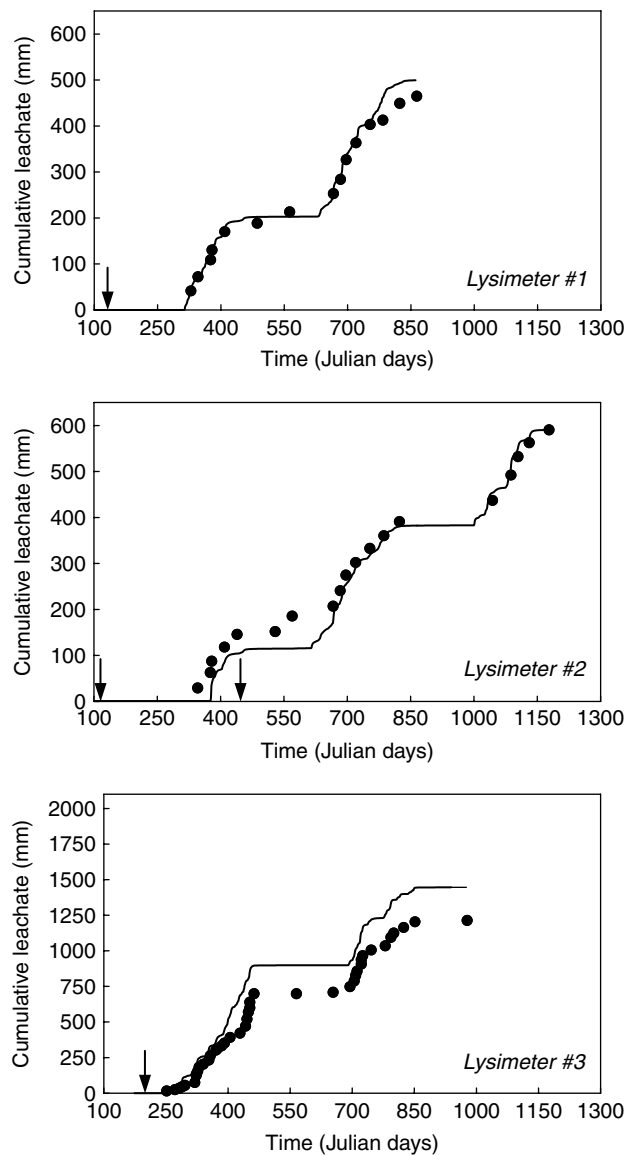


Figure 1. Comparison between observed cumulative volumes of leachate and those predicted by PESTRAS after a trial-and-error calibration. Black dots indicate observed data and the solid lines represent PESTRAS predictions. Arrows indicate the application dates. Day 1 is 1 January.

extent to an under-estimation of water fluxes (Fig 1). The maximum concentration in leachate from lysimeter 2 was under-estimated by a factor of 1.6, but total loads were closely matched (Table 4). Bentazone leaching through lysimeter 3 was considerably over-estimated by the model (Table 4), with the predicted maximum concentration in leachate being 18 times larger than that observed (Fig 2). It is not clear why such a large discrepancy was found for this particular lysimeter.

With the exception of lysimeter 1, the model was unable to predict the maximum concentrations, patterns of leaching or cumulative loads of bentazone using median sorption and degradation values, even though water balances for the three lysimeters were calibrated to some extent. The discrepancy between PESTRAS predictions and leaching data may be attributed to (1) an inadequate setting of the model

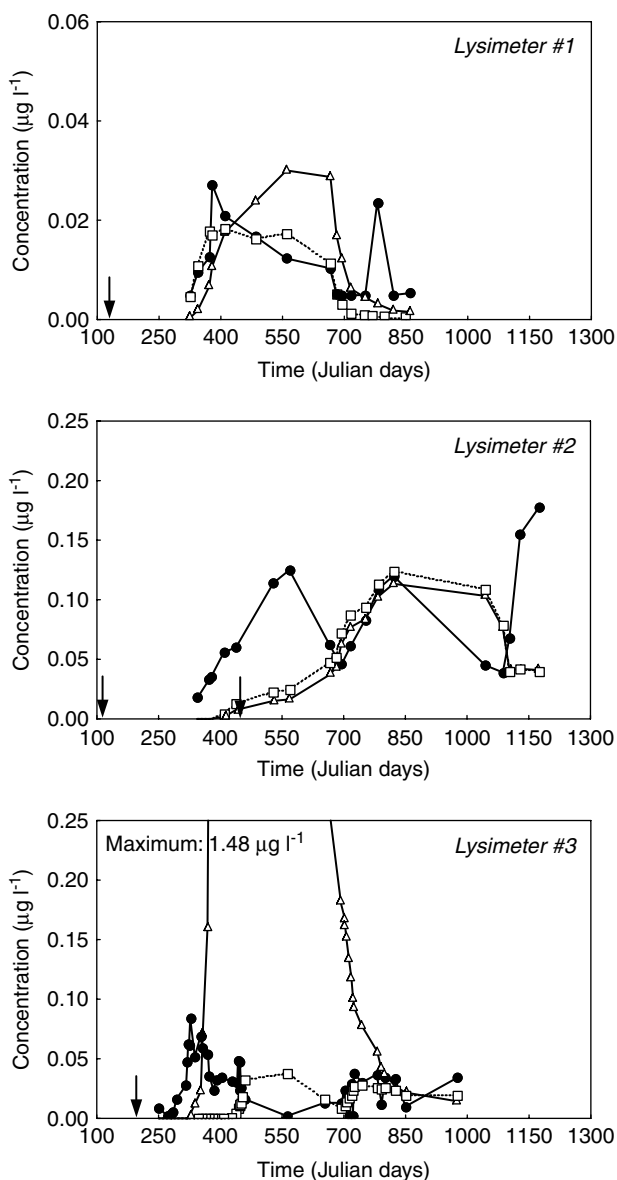


Figure 2. Comparison between (●) observed herbicide concentrations in leachate, (Δ) those predicted by PESTRAS using median DT_{50} and K_{om} values and (□) those predicted by PESTRAS after calibration by inverse modelling. Arrows indicate the application dates. Day 1 is 1 January.

input parameters affecting pesticide transport; (2) the use of sorption and degradation data which are not specific to the soils in each lysimeter; and (3) the possible failure of sub-routines influencing pesticide

transport in PESTRAS (eg water transport, soil temperature) to describe the fate of the herbicide in some particular lysimeters.

3.2 Herbicide leaching after calibration of K_{om} and DT_{50}

Calibrated parameters obtained by inverse modelling are reported in Table 5. PEST supplied calibrated parameters which were different from the starting values for all three lysimeters. None of the calibrated values for K_{om} and DT_{50} were at the upper (10^{10}) or lower (10^{-10}) limits of variation which were supplied to the inverse modelling package, and calibrated values were considered reasonable. Both parameters were found to significantly influence model predictions within the inverse modelling exercise. Calibrated K_{om} values ranged from 9.8 to 32.2 $ml\ g^{-1}$, whilst DT_{50} values ranged from 11.0 to 21.7 days. Calibrated values were markedly different from the starting values for lysimeters 1 and 3. The results, and the uncertainty associated with them, are within the range of variation reported for laboratory experiments for bentazone (K_{om} range 4–102 $ml\ g^{-1}$, DT_{50} range 7–87 days; Table 3). Calibrated values for K_{om} and, to a lesser extent, DT_{50} were significantly larger for the lysimeter situated in Schmallenberg than for those situated in Limburgerhof. Differences in status and management of the lysimeters, such as weather conditions, initial soil moisture status and cropping, might have contributed to the observed relationship between calibrated parameters and experimental location. Although 95% confidence ranges for calibrated values were relatively small for most lysimeters (Table 5), large correlations between the two calibrated parameters were reported in the PEST output file for two of the three lysimeters ($r > 0.98$). Parameter correlation is common in environmental modelling, although it is often overlooked when manual approaches to calibration are used.² Large correlation between optimised parameters is likely to result in non-uniqueness of calibration results. Non-uniqueness, non-identifiability and instability can all contribute to the ill-defined nature of inverse problems²⁵ and may result in solutions that are meaningless from a practical perspective.²⁶ Issues of non-uniqueness are investigated in detail below.

Concentrations for bentazone predicted using calibrated K_{om} and DT_{50} values are compared with

Table 4. Maximum bentazone concentrations in leachate and cumulative loads predicted by PESTRAS before and after automatic calibration by inverse modelling

Lysimeter number	Maximum concentrations ($\mu g\ litre^{-1}$)			Cumulative load ($mg\ m^{-2}$)		
	Observed ^a	Simulated prior to calibration	Simulated after calibration	Observed	Simulated prior to calibration	Simulated after calibration
1	0.027	0.030	0.018	0.005	0.005	0.004
2	0.178	0.114	0.124	0.043	0.037	0.040
3	0.084	1.480	0.038	0.038	0.667	0.015

^a Maximum concentration in any single leaching event; annual average concentrations were $<0.1\ \mu g\ litre^{-1}$.

Table 5. Initial and calibrated values for K_{om} and DT_{50}

Lysimeter number	K_{om} (ml g ⁻¹)		DT_{50} (days)		Sum of squared residuals		Number of runs ^b	Correlation ^c
	Initial	Calibrated ^a	Initial	Calibrated ^a	Before calibration	After calibration		
1	16.4	9.8 (7.2–12.0)	17.8	11.0 (8.9–13.2)	1.73×10^{-3}	7.80×10^{-4}	64	0.988
2	16.4	15.7 (8.4–23.0)	17.8	17.4 (11.2–23.5)	6.74×10^{-2}	6.58×10^{-2}	18	0.981
3	16.4	32.2 (32.1–32.3)	17.8	21.7 (21.7–21.7)	1.83×10^1	4.44×10^{-2}	44	0.328

^a 95% confidence limits of calibrated parameters in parentheses.

^b Number of PESTRAS runs carried out for each calibration.

^c Correlation coefficients between K_{om} and DT_{50} as returned by PEST.

observed data in Fig 2 and maximum concentrations and loads are presented in Table 4. The calibration did not result in an improvement in the prediction of the maximum concentration and total load for lysimeter 1 (Table 4), although the shape of the breakthrough curve (Fig 2) was improved and the overall sum of squared residuals was reduced (Table 5). Calibration gave only a slight improvement over median K_{om} and DT_{50} values for lysimeter 2 (Fig 2), the shape of the breakthrough curve being mis-matched by the model even with the calibrated parameters. In contrast, the use of calibrated parameters generated a much improved fit to experimental data for lysimeter 3. A number of reasons can be proposed to explain the discrepancy between observations and PESTRAS predictions for lysimeter 2 and the lack of improvement provided by the use of calibrated parameters. First, this might be attributed to the inherent variability in the analysis of pesticide concentrations at low residue levels. Although analytical determinations were carried out according to best laboratory practice, laboratory data are always subject to uncertainty.²⁷ Second, some processes not included in the PESTRAS model, such as preferential flow or time-dependent sorption, might significantly affect the fate of the herbicide, or the mechanisms implemented into the model may be inappropriate to predict the time series of concentrations that were observed in this lysimeter. Third, other parameters not included in the calibration exercise, especially those which greatly influence model predictions, may be vital in describing the breakthrough curve shown in Fig 2. This might include the Freundlich exponent, which is one of the parameters that most influences pesticide losses in PESTRAS,¹⁶ but also parameters related to dispersion within soil or to the variation of pesticide degradation with depth. In addition, default values for the calculation of derivatives and convergence and termination criteria supplied in PEST may be inadequate for this particular dataset, resulting in failure of the inverse modelling package to achieve convergence.

3.3 Influence of n_f values on calibration results

Inverse modelling exercises involving the calibration of K_{om} and DT_{50} were conducted for different n_f values. The number of model runs required to cause PEST

to end calibration ranged between seven and 98. The latter number was obtained for an n_f value of 1.06 for lysimeter 3. Scenarios where only seven model runs were necessary to end calibration reflected the lack of sensitivity of the goodness-of-fit function to variations in K_{om} and DT_{50} applied by PEST. This occurred for all three lysimeters for small values of n_f (ie $n_f < 0.67$). Figures 3 to 5 present calibration results for different n_f values for lysimeters 1, 2 and 3, respectively (only those final calibrated values which differed from the starting values supplied to PEST are shown). For all lysimeter datasets, the use of different n_f values resulted in different combinations of calibrated K_{om} and DT_{50} values, thereby reflecting the significant sensitivity of PESTRAS to the Freundlich exponent.¹⁶

For lysimeter 1 (Fig 3), the use of different n_f values resulted in larger DT_{50} values being compensated by smaller K_{om} values in the calibration (Pearson $r = 0.78$, $P < 0.01$). An increase in n_f value resulted in a decrease in DT_{50} ($P < 0.01$) and an increase in K_{om} ($P < 0.01$). The variation of calibrated K_{om} values against n_f followed a clear exponential relationship ($r^2 = 1.00$, $P < 0.01$), reflecting the mathematics of the Freundlich equation which is used to describe pesticide sorption in PESTRAS (eqn (1)). All combinations of K_{om} and DT_{50} presented in Fig 3 successfully calibrated the PESTRAS model for the different n_f values used. A decrease in the Φ function which represents the lack-of-fit between the model and the lysimeter data was obtained by lowering the n_f value and calibrating the model against K_{om} and DT_{50} . Below an n_f value of 0.78, PEST returned the starting values supplied, reflecting the inability of the package to calibrate the model for small values of this parameter. The relative change in the Φ function for the calibrations was small (maximum variation 4.0%) although the variation of n_f applied was significant. This stability was reflected in the pesticide breakthrough curves being similar for the different combinations of calibrated K_{om} and DT_{50} (Fig 6).

Results for lysimeter 2 (Fig 4) contrasted with those obtained for lysimeter 1 in that: (1) the correlation between calibrated K_{om} and DT_{50} values for the different n_f values was positive (Pearson $r = 0.79$, $P < 0.01$); (2) the use of larger Freundlich values resulted in larger calibrated DT_{50} values (Pearson $r = 0.66$, $P = 0.06$); and (3) smaller values of the

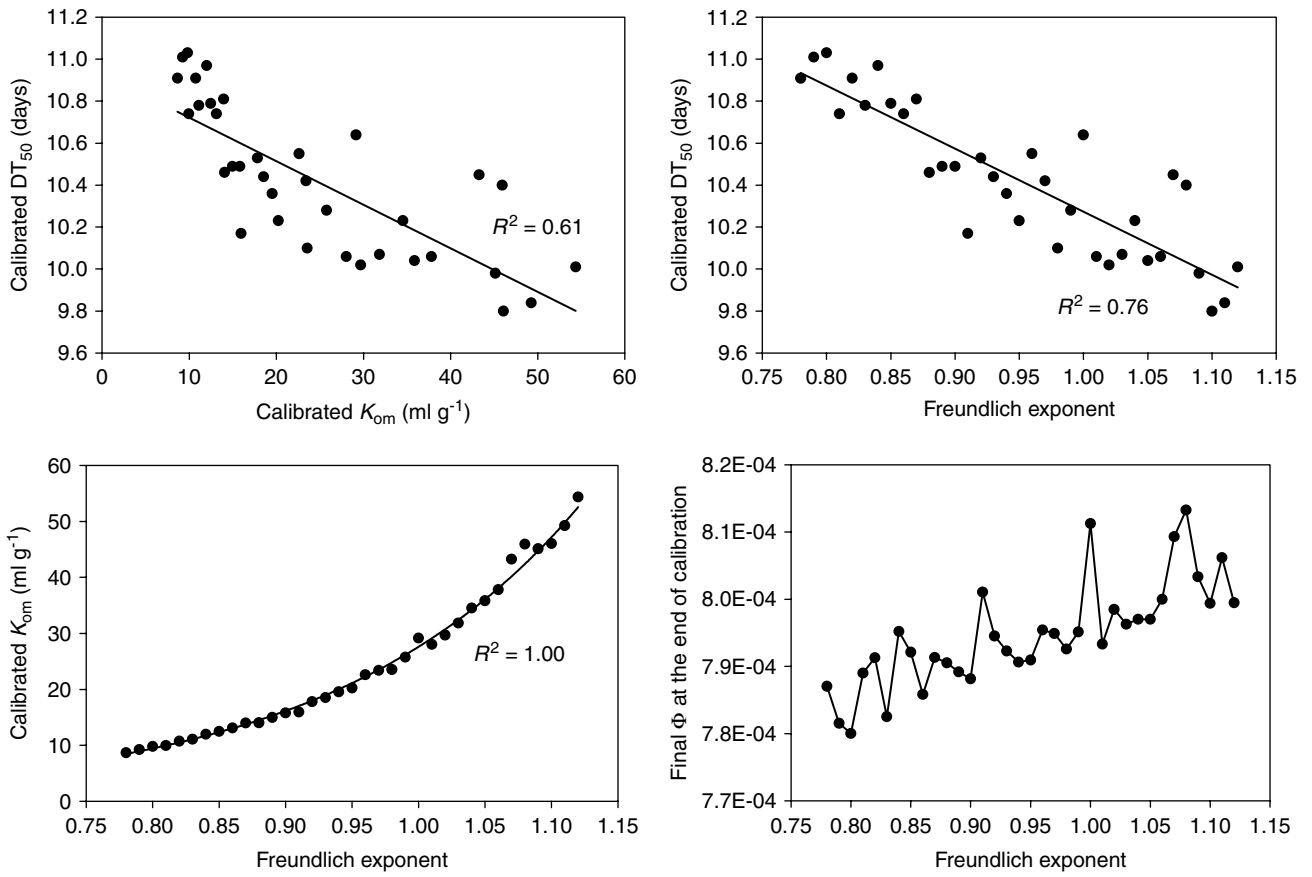


Figure 3. Calibration results for different values of n_f for lysimeter 1.

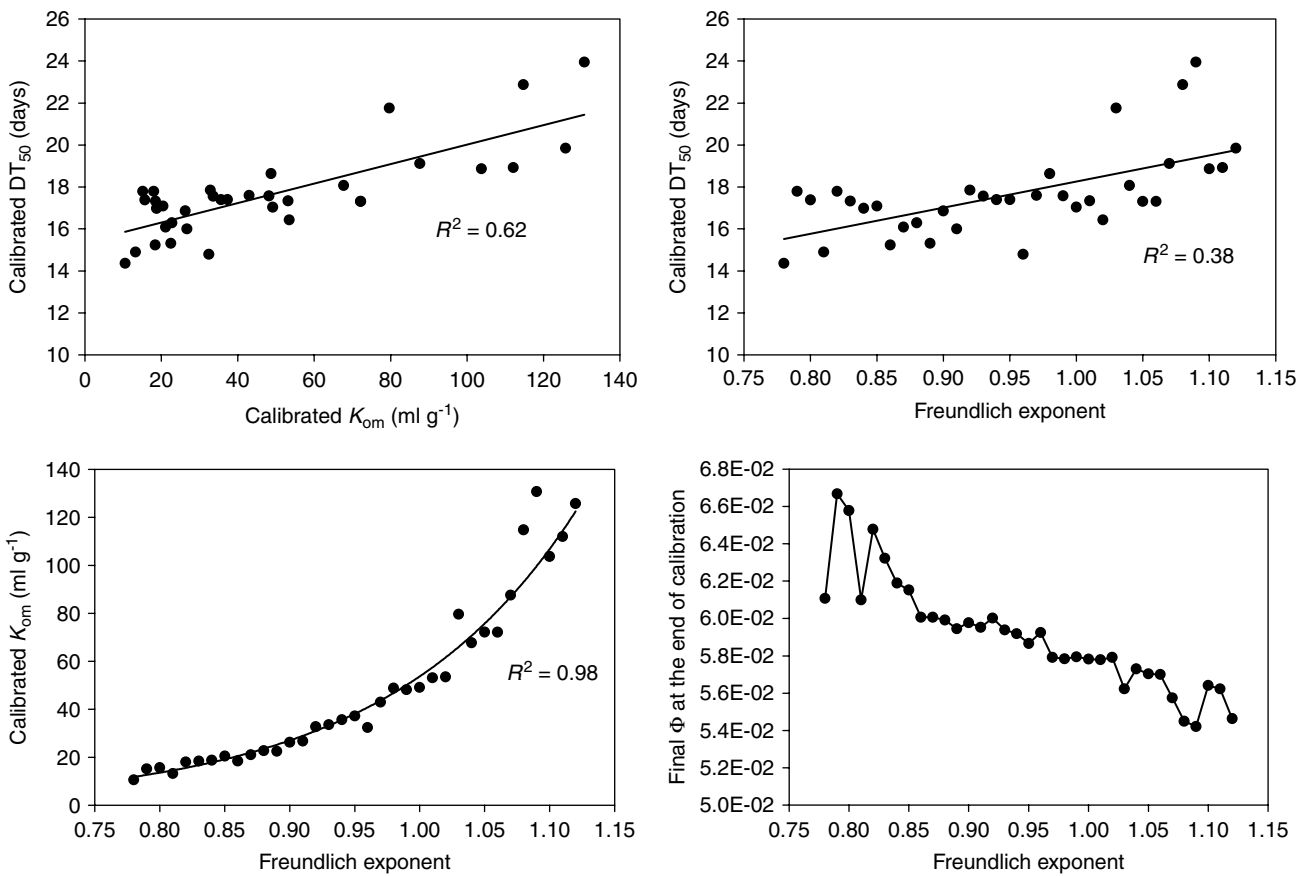


Figure 4. Calibration results for different values of n_f for lysimeter 2.

Φ function (ie improved fit to the simulated data) were obtained when larger n_f values were used. As for lysimeter 1, an exponential relationship between calibrated K_{om} and n_f values was found, although deviations from the curve were more frequent and larger than for the first dataset. These deviations may reflect the difficulty encountered by PEST in finding the minima of the Φ function for a number of modelling scenarios corresponding to specific values of n_f . Pesticide breakthrough curves obtained using the calibrated parameter values were more scattered than those for lysimeter 1 (Fig 6), although the overall shape remained similar for all calibrations.

Results for lysimeter 3 provided a third behaviour with respect to the influence of n_f values on calibrated values for K_{om} and DT_{50} (Fig 5). For n_f values <0.82 and >0.87 , calibrated DT_{50} values were relatively constant when n_f was varied. Calibrated values were 21.2–22.3 days and 6.3–6.4 days for $n_f < 0.82$ and $n_f > 0.87$, respectively. The grouping was also reflected in calibrated values for K_{om} which were distributed along two exponential curves when plotted against n_f . The chart plotting the Φ function against n_f showed that two types of Φ values were obtained, depending on the value of n_f . These differences were reflected in different calibrated pesticide breakthrough curves (Fig 6). In some instances, the calibration of PESTRAS resulted in the model not simulating the first increase in concentrations (day 271 to day 461) and over-estimating measured concentrations

from day 450 to day 562. The magnitude of concentrations from day 694 was somewhat better simulated, although the model failed to simulate the low concentrations in leachate collected on day 792 and 850. The associated Φ values were $ca 1.8 \times 10^{-2}$. Pesticide breakthrough curves which corresponded to smaller Φ values were those which provided a good fit to the initial increase in concentrations in leachate, but then failed to simulate the presence of the compound in leachate from day 450 onwards (Fig 6). A range of intermediate curves between the two broad groupings described above were obtained in a small number of cases. Occasionally, an increase in n_f value by 1 unit (eg from $n_f 0.94$ to $n_f 0.95$ or from $n_f 0.95$ to $n_f 0.96$) resulted in calibrated K_{om} and DT_{50} values providing very different pesticide breakthrough curves.

The use of different values for n_f resulted in the derivation of different calibrated values for K_{om} and DT_{50} for all three lysimeters. Different types of behaviour with regard to calibration were identified for the three lysimeter datasets used. In some instances (eg lysimeter 1), K_{om} and DT_{50} compensated for each other and different calibrated K_{om} – DT_{50} combinations resulted in similar predictions of pesticide breakthrough. In contrast, lysimeter 3 demonstrated that variations in n_f values may result in calibrated K_{om} – DT_{50} combinations which lead to different pesticide breakthrough curves. The selection of a range of adequate values for n_f for lysimeter 3 may be based on a visual assessment of pesticide

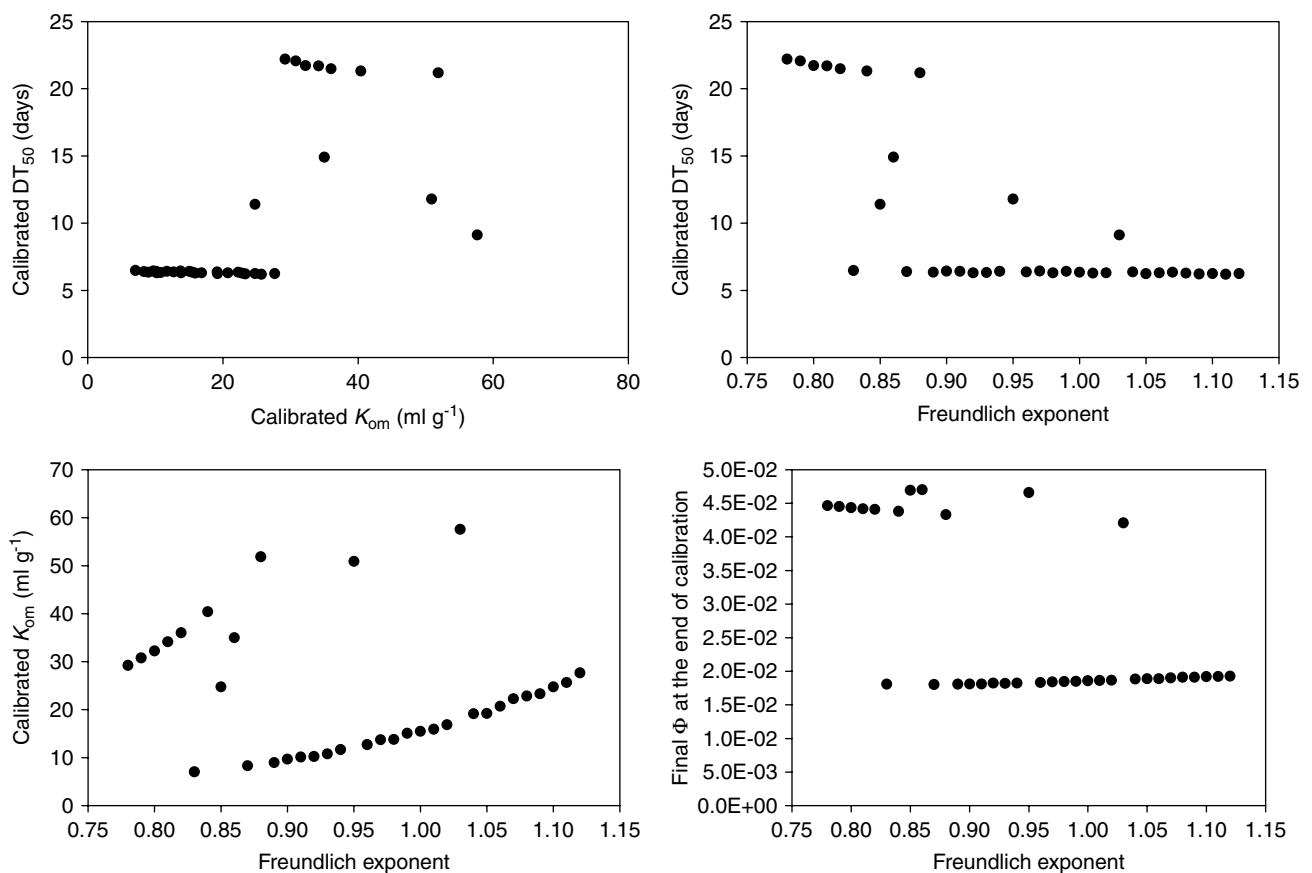


Figure 5. Calibration results for different values of n_f for lysimeter 3.

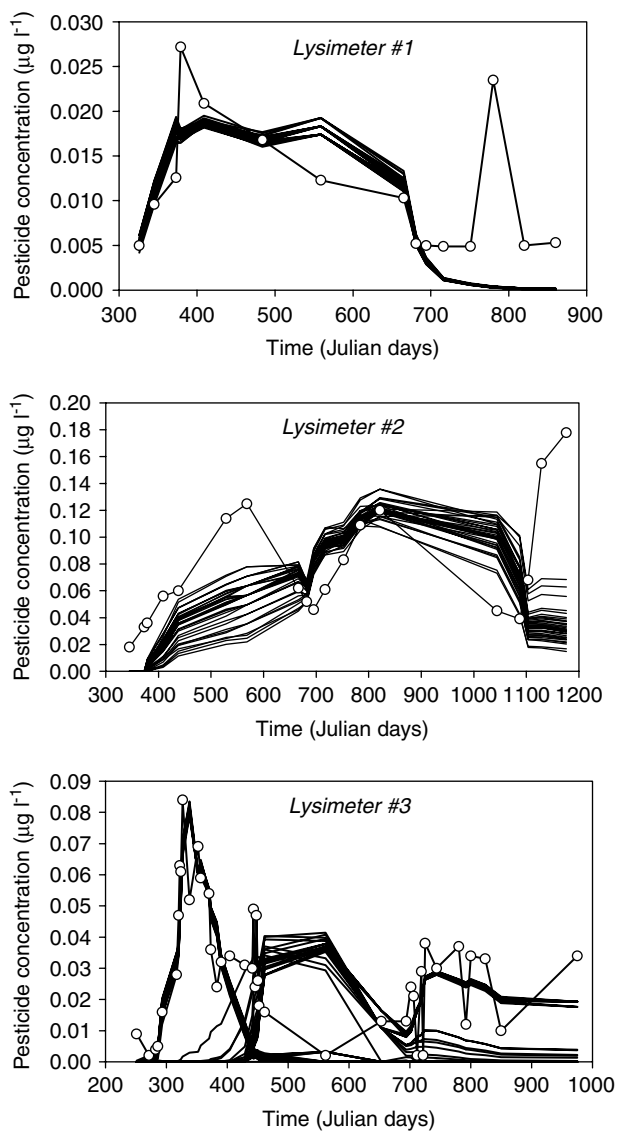


Figure 6. Pesticide breakthrough simulated after calibration of PESTRAS for different n_f values (plain lines). The measured data are represented by open circles.

breakthrough curves, although this process is likely to be subjective. Selecting a value for n_f on the basis of the calibration results for lysimeter 1 is made difficult by the derivation of similar pesticide breakthrough curves for different n_f values (Fig 6). The examination of the variation of the overall goodness-of-fit (Fig 3) provided little help for the selection of an n_f value (and hence a K_{om} - DT_{50} combination) since the Φ function increased monotonously with increasing n_f (a monotonic decrease was found for lysimeter 2; Fig 4). Such a selection would have been possible if the Φ function had shown a clear minimum within the range of n_f values covered here.

3.4 Influence of starting values on calibration results

A total of 225 combinations of K_{om} and DT_{50} starting values were supplied to PEST for each of the three lysimeter datasets and this resulted in a total of 675 automated PESTRAS calibrations and 27 159 model

runs. Calibrated K_{om} and DT_{50} values are presented in Fig 7 and resulting pesticide breakthrough curves simulated by the model are shown in Fig 8. The grid nodes in Fig 7 correspond to the 225 initial combinations of starting values supplied to PEST.

Calibration results were dependent on starting values for lysimeter 1 (Fig 7). For combinations of K_{om} and DT_{50} starting values falling below the 1:1 line, most calibrations were unsuccessful, and starting values were returned by PEST at the end of the calibration. However, two convergence zones were identified. The first zone corresponds to very small K_{om} values with DT_{50} values in the range 1.3–4.4 days. Most of the K_{om} values were at the lower bound of variation which was supplied to PEST (10^{-10}). These K_{om} values are clearly not reasonable. The second convergence zone was fairly

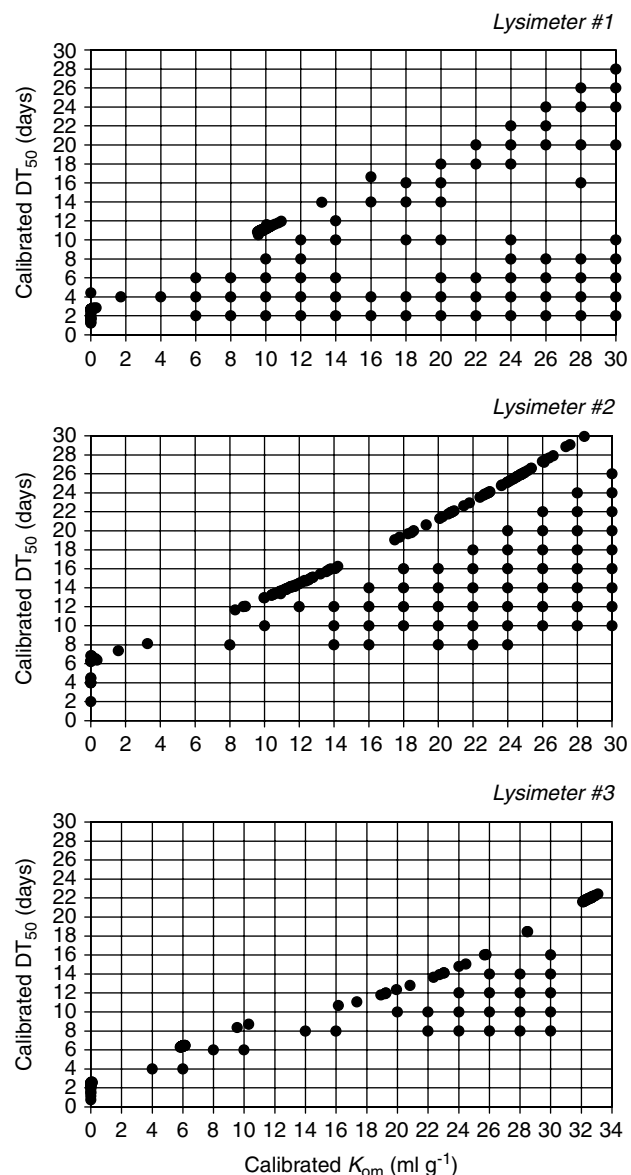


Figure 7. Combinations of calibrated K_{om} and DT_{50} values obtained for different starting values. Calibrated values are represented by closed circles. Each grid node corresponds to a combination of starting values.

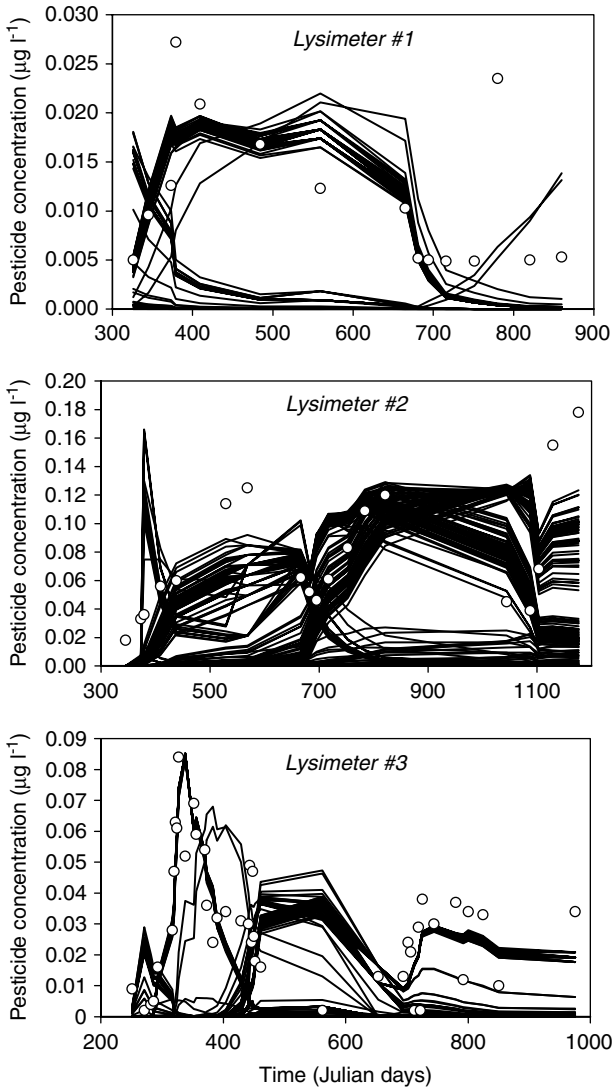


Figure 8. Populations of pesticide breakthrough curves obtained for calibrations carried out with different starting values. The measured data are represented by open circles.

small in the parameter space, and was defined by the following values for K_{om} and DT_{50} : $9.6 < K_{om} < 10.7$ and $10.8 < DT_{50} < 12$. Only five combinations of calibrated values did not fall into any of these three categories. Combinations of starting values were classified on the basis of the calibration results (Fig 9). The Figure shows that calibration results were likely to fall into the first convergence zone if starting values were below the 1:1 line, while combinations of starting values situated above the 1:1 line resulted in calibrated values in the second convergence zone. Calibrations in the second convergence zone provided very similar pesticide breakthrough curves (Fig 8). Curves which gave little resemblance to the experimental data in Fig 8 were those corresponding to the first convergence zone with small K_{om} values.

Four types of calibration behaviour were identified for lysimeter 2 on the basis of the position of the combination of starting values in the parameter space. For starting combinations falling below a regression line between K_{om} and DT_{50} (Fig 7), PEST either

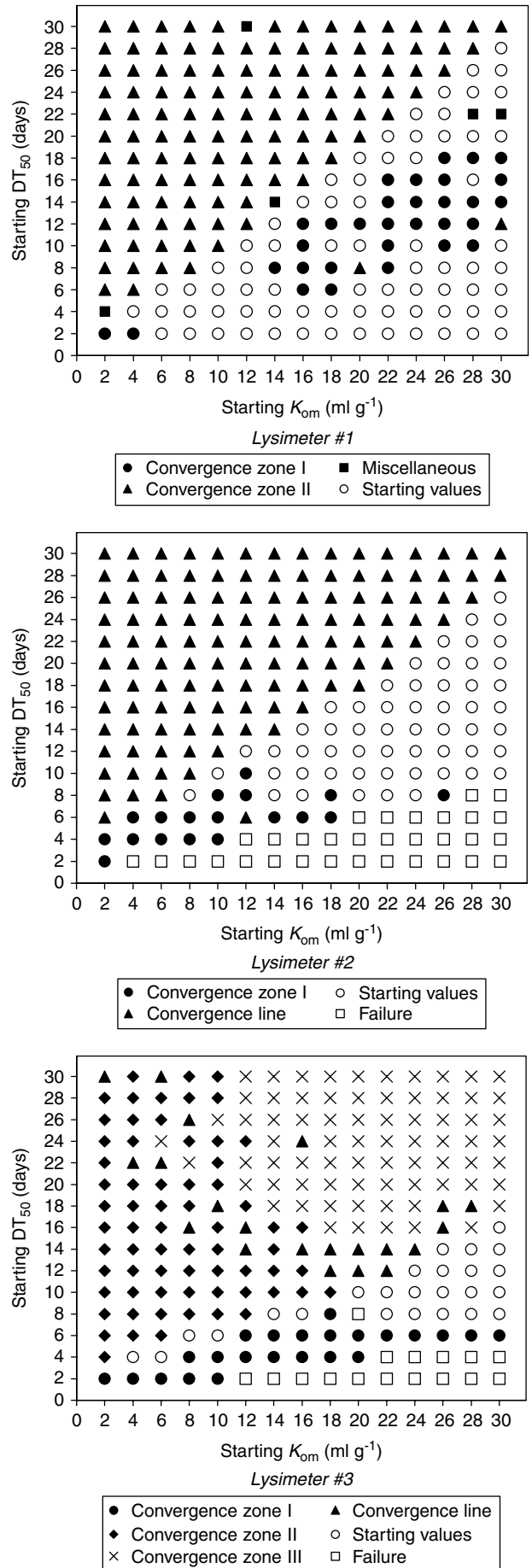


Figure 9. Dependence of the calibration outcome on the position of starting values in the K_{om} - DT_{50} space.

returned starting values or very small values for K_{om} and DT_{50} , or failed to provide calibration results because the gradient of the Φ function became zero. As for lysimeter 1, calibration was only successful for combinations of starting values above a particular line (Figs 7 and 9), but in this instance, calibrated values for K_{om} and DT_{50} fell onto a curve (Fig 7) rather than being concentrated in a convergence zone. Pesticide breakthrough curves corresponding to these calibrated values varied significantly (Fig 8) although, numerically, the 117 calibrations falling on this line provided a very similar fit to the data (Φ values 0.060 to 0.069; data not shown).

Lysimeter 3 showed a complex behaviour when compared with the other two datasets. Again, depending on the combination of starting values (Fig 7), the following results could be obtained (Fig 9): failure to calibrate because of an insensitivity of the Φ function to K_{om} and DT_{50} ; the return of starting values; a first convergence zone with small values of K_{om} ; a second convergence zone regrouping 63 calibrations defined by $5.8 < K_{om} < 6.2$ and $6.3 < DT_{50} < 6.5$; a third convergence zone regrouping 89 calibrations defined by $32.1 < K_{om} < 33.1$ and $21.6 < DT_{50} < 22.4$; and a convergence curve that was less well defined than for lysimeter 2. Calibrations which provided a good fit to the first peak in pesticide breakthrough were related to the second convergence zone. Calibrations belonging to the third zone yielded pesticide breakthrough curves which were closer to the data from day 650 onwards (Fig 8). The final values of the Φ function were 0.180 and 0.048 for the second and third convergence zones, respectively.

3.5 Response surface analysis

Forward modelling for multiple combinations of K_{om} and DT_{50} was undertaken to try to understand the difference in calibration behaviour shown by the three lysimeter datasets in relation to the use of different starting values for K_{om} and DT_{50} . For lysimeters 1 and 2, values of K_{om} and DT_{50} were modified between 2 and 30 ml g^{-1} , and between 2 and 30 days, respectively, using a one-unit increment step for both parameters. Ranges of variation were 2–40 ml g^{-1} and 2–40 days for lysimeter 3 because earlier investigations related to starting values had suggested a convergence zone for values of $K_{om} > 30 \text{ ml g}^{-1}$ and $DT_{50} > 30$ days (data not shown). The sum of squared residuals between the simulated and measured concentration data (the Φ statistics) was calculated for each run. Figure 10 presents surface and contour plots of the variation of the reciprocal of the Φ statistics for all combinations of K_{om} and DT_{50} for all three lysimeters. In the plots, the best fit to the experimental data is obtained for the smallest values of Φ (a lack-of-fit statistic) hence the largest values of Φ^{-1} (a goodness-of-fit statistic) in Fig 10.

Figure 10 for lysimeter 1 shows that, within the parameter space explored, the goodness-of-fit surface has two flat regions divided by a ridge. The flat section

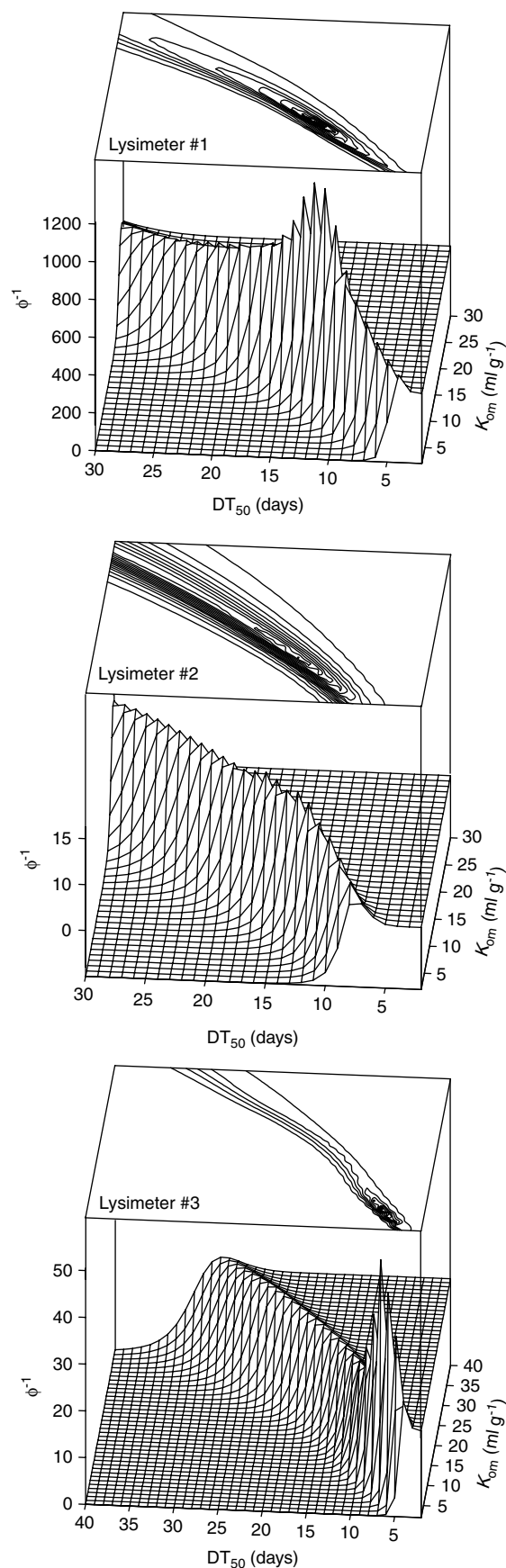


Figure 10. Surface and contour plots showing the goodness-of-fit to the experimental data (Φ^{-1}) for multiple combinations of K_{om} and DT_{50} . Each grid node represents a PESTRAS run for the corresponding combination of K_{om} and DT_{50} . The saw tooth pattern on the ridges has been artificially created by the plotting software used.

for low K_{om} values (bottom left corner of Fig 10) corresponds to those combinations of K_{om} and DT_{50} which resulted in a large overestimation of pesticide concentrations in leachate, while the other flat section (top right corner of Fig 10) corresponds to those values of K_{om} and DT_{50} which resulted in negligible leaching predicted by PESTRAS. The Φ^{-1} function for these latter runs thus equalled the sum of the reciprocal of the squared measured concentrations ($\Phi^{-1} = 371$). The parameter space was divided by a ridge with steep slopes which reflected the large sensitivity of Φ^{-1} in this region of the parameter space. A peak clearly identifiable on the contour plot in Fig 10 was observed for approximately $K_{om} 10 \text{ ml g}^{-1}$ and DT_{50} 11 days, which is consistent with the convergence zone observed for the calibration of lysimeter 1 (Table 5; Fig 7). No large increase in the Φ^{-1} statistics was observed for very low values of K_{om} , which confirms that convergence zone I in Fig 7 is an artefact created by PEST. This resulted from PEST assigning a value of 10^{-10} to calibrated K_{om} , the value which was supplied as the minimum bound of variation for K_{om} . PEST was unable to calibrate PESTRAS in those specific instances. When investigating the influence of starting values on calibration results, a number of calibrations resulted in PEST returning the starting values (Fig 7) since the package found that the ' Φ gradient [was] zero'. This lack of sensitivity of Φ^{-1} corresponded to flat portions of the error surface in the top right sections of Fig 10.

Results of PESTRAS runs obtained for lysimeter 2 were similar to those for lysimeter 1 in that two flat sections were separated by a ridge. However, surface and contour plots for lysimeter 2 suggest that there was no clear maximum on this crest. Instead, the contour plot suggests that very similar Φ^{-1} values could be obtained for a large number of combinations of K_{om} and DT_{50} . These results are consistent with those obtained earlier where multiple combinations of calibrated values falling on a line were returned by PEST when different starting values were supplied (Fig 7).

In common with results for lysimeters 1 and 2, the K_{om} - DT_{50} parameter space was divided into two flat sections and a ridge for lysimeter 3 (Fig 10). There was a sharp increase in Φ^{-1} around values of K_{om} of 6 ml g^{-1} and DT_{50} of 7 days corresponding to a clear convergence zone (Fig 7), but, in contrast to lysimeter 1, the rest of the Φ^{-1} values situated on the ridge were similar (Fig 10). This can be best observed on the contour plot. These patterns are consistent with the existence of convergence zone II in Figs 7 and 9 and the presence of a convergence curve (Fig 7). As for the other two lysimeters, convergence zone I (Figs 7 and 9) appears to be an artefact reflecting the inability of PEST to calibrate PESTRAS for specific starting values. A local maximum of the Φ^{-1} function corresponding to the third convergence zone (ie $32 < K_{om} < 34 \text{ ml g}^{-1}$ and $20 < DT_{50} < 24$ days) could be identified on the ridge although the 3D

positioning of Fig 10 selected for presentation does not allow the identification of the small increase in the Φ^{-1} values.

4 DISCUSSION

Investigations on the influence of the value attributed to the Freundlich exponent n_f (a parameter not included in the initial calibrations) revealed that different calibrated K_{om} - DT_{50} combinations describing the experimental data equally well could be obtained for different n_f values. The K_{om} parameter compensated for changes in the values of n_f . Calibration results could not be used to select an adequate value for n_f from a range of possible values, since the goodness-of-fit monotonically increased or decreased with increasing n_f values. Adding n_f to the list of parameters to be optimised is not a viable option since K_{om} and n_f would compensate for one another within the calibration, and this would lead to an ill-defined calibration problem. It is therefore suggested that, provided K_{om} , DT_{50} and n_f are the most influential parameters on the prediction of pesticide concentrations:^{10,11} (1) calibrations against pesticide leaching in lysimeter experiments are restricted to the parameters K_{om} and DT_{50} , keeping in mind that non-uniqueness issues can be encountered; and (2) a number of calibrations are carried out for different n_f values. The latter point will help to assess the confidence that should be attributed to K_{om} and DT_{50} values derived by inverse modelling.

For the three lysimeters, the calibration behaviour for K_{om} and DT_{50} was dependent on the location of the K_{om} - DT_{50} starting values in the parameter space. Combinations of starting values falling below a line in a DT_{50} versus K_{om} plot led to a failure to calibrate (ie return of starting values after a few runs or setting of K_{om} to the smallest value as specified in the possible variation range). A number of reasons can be put forward to explain the fact that PEST failed to find the convergence zones for these starting combinations. First, default values for derivative calculation and termination settings provided in PEST were used in the calibration. These default settings might be inadequate for the present inverse modelling problem and adjustment might achieve more consistent results. Second, the implementation of the Gauss-Levenberg-Marquardt in PEST might be inadequate for dealing with the present calibration problem where large portions of the error surfaces showed little sensitivity to changes in parameter values. The type of behaviour revealed here by response surface analysis would provide a challenge to any algorithm for non-linear estimation, and the performance of other inverse modelling packages, such as UCODE,⁶ SUFI²⁸ or SUSE,²⁹ therefore needs to be assessed. UCODE and SUSE implement modified versions of the Gauss-Newton and Simplex algorithms, respectively, while SUFI is based on a forward, sequential and iterative approach which can

be integrated within a Bayesian framework. Third, the computation of derivatives of all observations with respect to all adjustable parameters might not be accurate enough to permit a robust implementation of the Gauss–Levenberg–Marquardt procedure. The presence of round-off errors incurred in the calculation of derivatives is the most common cause of PEST failure to achieve a robust calibration.⁵ Accuracy of the derivatives will be mainly dependent on the accuracy of the resolution of differential equations by PESTRAS and on the rounding of PESTRAS predictions in the model output. Inaccuracies resulting from these two sources will aggregate. PESTRAS has been developed for simulation purposes and is not optimised for inverse modelling applications. Dedicated model codes and procedures for parameter estimation may have to be developed to obtain reliable model derivatives and robust estimates of K_{oc} and DT_{50} .³⁰

For combinations of starting values other than those which returned starting values, calibration behaviour was dependent on the dataset considered. In some instances, starting combinations led to a more or less unique set of calibrated parameters, as in lysimeter 1. In other cases, calibration results were not unique and a range of K_{om} and DT_{50} values were returned. Again, the failure to return a unique combination of parameters might be attributed to an inadequate parameterisation of PESTRAS or PEST, the lack of precision in the calculation of derivatives, but also to the fact that the pesticide concentration data used might not enable the derivation of a unique K_{om} – DT_{50} combination. A parallel can be drawn with the field of soil water physics where inverse modelling has been used to assess soil hydraulic properties from column experiments.³ The use of water outflow data alone will lead to non-uniqueness issues in the calibration, but the integration of additional data (eg tensiometric measurements) will make the calibration problem better posed. Limitations resulting from the use of leaching data alone for estimating sorption and degradation data for pesticides have already been expressed by Heistermann *et al*³¹ on the basis that the monitoring of leaching water does not differentiate between different flow domains. Further research is required into the identification of the data requirements for a robust calibration of the water and pesticide components of leaching models. This might best be achieved through response surface analysis³² and optimal experimental design which enables the identification of data requirements for a well-posed calibration problem prior to conducting experiments. In the present study, the presence of a large number of combinations of K_{om} and DT_{50} providing a similar goodness-of-fit to the data implies that the inverse modelling approach may not be applicable to all combinations of lysimeter data and leaching models.

The examination of 3D charts plotting Φ or Φ^{-1} against K_{om} and DT_{50} following forward modelling

was useful in explaining the different calibration behaviours observed earlier. The plotting of the error surface as a stand-alone activity (ie without recurring to inverse modelling packages) could be of more general interest for identifying instances where there is no clear global minimum of the Φ function in the calibration of pesticide leaching models, and hence where non-uniqueness in optimisation using inverse modelling packages is likely. Provided the grid extends over large ranges of K_{om} and DT_{50} values and the grid mesh is fine enough, this approach provides a way to easily identify whether a convergence zone exists and its location in the parameter space, thereby negating the need to resort to inverse modelling procedures. The approach thus provides a practical solution to non-uniqueness issues where pesticide leaching models are used to estimate K_{om} and DT_{50} values. It was effective in terms of running time when compared with the investigation of the influence on calibration results of using different starting values as presented earlier in this paper. The main limitations are that (1) only two parameters can be considered for an easy visual assessment of the error surface in three dimensions and (2) the technique should be restricted to those models with a short running time, ie a few seconds to a few minutes. Here, response surface analysis helped to characterise the correlation in the modelling between the parameters K_{om} and DT_{50} , which resulted in calibration non-uniqueness. Poeter and Hill² suggest two approaches for dealing with large correlation between parameters. The first is to collect and include in the calibration additional data that will uniquely define all parameter values. Investigations with regard to data requirements for ensuring a robust calibration of pesticide leaching models are desirable. The second option to address correlation issues is to set one of the parameters to a given value and estimate the other. This approach cannot be implemented in the present situation since both K_{om} and DT_{50} are uncertain parameters and one would not have any confidence in assigning a particular value to either parameter.

5 CONCLUSIONS

Experimental data collected during field or semi-field leaching studies can be used to derive sorption and degradation values through automated calibration of an appropriate pesticide leaching model. Such an approach is expected to be of interest for: (1) simulating pesticide fate in those cases where soil-specific sorption and degradation data are not available; (2) identifying instances in which the use of laboratory values in modelling fails to describe field behaviour, and to derive alternative values in those circumstances; and (3) extrapolating results to other climatic conditions as degradation rates derived through inverse modelling are corrected for influences of fluctuations in temperature and moisture and can be tied to reference conditions.

The present research demonstrated that sorption and degradation values derived through calibration of a model against pesticide leaching data should be examined with care. Investigations revealed that calibration results were significantly influenced by the starting values provided to the inverse modelling package and by values attributed to an influential parameter not included in the calibration exercise. Response surface analysis, the examination of the error surface between observed and predicted values through forward modelling, proved a useful tool in (1) identifying those instances where non-uniqueness is likely to occur in the calibration; (2) assessing the overall confidence that should be assigned to calibration results; and (3) finding optimised values for parameters without resorting to inverse modelling procedures. Further research is required into the identification of the data requirements for a robust calibration of the water and pesticide components of leaching models through inverse modelling.

Within the context of pesticide registration, average or median laboratory values will remain the primary input at lower tiers of regulatory modelling. Values derived through inverse modelling should be regarded as additional information helping to build an overall picture of how a crop-protection product is likely to behave once released into the environment.

ACKNOWLEDGEMENTS

The authors gratefully acknowledge the funding of this work and the provision of the lysimeter data by BASF AG.

REFERENCES

- Dubus IG, Beulke S and Brown CD, Calibration of pesticide leaching models: critical review and guidance for reporting. *Pest Manag Sci* 58:745–758 (2002).
- Poeter EP and Hill MC, Inverse models: a necessary next step in ground-water modeling. *Ground Water* 35:250–260 (1997).
- Hopmans JW and Šimunek J, Review of inverse estimation of soil hydraulic properties, in *Characterization and measurement of the hydraulic properties of unsaturated porous media*, ed by van Genuchten MT, Leij FJ and Wu L, University of California, California, pp 643–659 (1999).
- Beven K, *Rainfall-runoff modelling: the primer*, John Wiley and Sons Ltd, Chichester, UK (2001).
- Doherty J, *PEST—Model independent parameter estimation*, Watermark Computing, Corinda, Australia (2000).
- Poeter EP and Hill MC, *Documentation of UCODE, a computer code for universal inverse modelling*, US Geological Survey, Water resources investigations report 98-4080 (1998).
- Janssen PHM and Heuberger PSC, Calibration of process-oriented models. *Ecol Model* 83:55–66 (1995).
- Roulier S and Jarvis NJ, Analysis of inverse procedures for estimating parameters controlling macropore flow and solute transport in the dual-permeability model MACRO. *Vadose Zone J* 2:349–357.
- Boesten JJTI, Sensitivity analysis of a mathematical model for pesticide leaching to groundwater. *Pestic Sci* 31:375–388 (1991).
- Dubus IG, Brown CD and Beulke S, Sensitivity analyses for four leaching models. *Pest Manag Sci* 59:962–982 (2003).
- Dubus IG and Brown CD, Sensitivity and first step uncertainty analyses for the preferential flow model MACRO. *J Environ Qual* 31:227–240 (2002).
- Walker A and Jurado-Exposito M, Adsorption of isoproturon, diuron and metsulfuron-methyl in two soils at high soil:solution ratios. *Weed Res* 38:229–238 (1998).
- Beulke S, Dubus IG, Brown CD and Gottesbüren B, Simulation of pesticide persistence in the field on the basis of laboratory data—a review. *J Environ Qual* 29:1371–1379 (2000).
- Gaillardon P, Fauconnet F, Jamet P, Soulas G and Calvet R, Study of diuron in soil solution by means of novel simple techniques using glass microfibre filters. *Weed Res* 31:357–366 (1991).
- Biologische Bundesanstalt für Land- und Forstwirtschaft (BBA), Guidelines for the testing of plant protection products in registration procedures. Part IV, 4–3: Lysimeter tests for the translocation of plant protection products into the subsoil, BBA, Braunschweig, Germany (1990).
- Tiktak A, van der Linden AMA and Swartjes FA, *PESTRAS: a one-dimensional model for assessing leaching and accumulation of pesticides in soil*, National Institute of Public Health and the Environment, Report no 715501003, Bilthoven, The Netherlands (1994).
- Tiktak A, van der Linden AMA and van der Pas LJT, Application of the Pesticide Transport Assessment Model to a field study in a humic sandy soil in Vredepeel, the Netherlands. *Pestic Sci* 52:321–336 (1998).
- van Genuchten MTH, A closed-form equation for predicting the hydraulic conductivity of unsaturated soils. *Soil Sci Soc Am J* 44:892–898 (1980).
- Tiktak A, van der Linden AMA and Merkelbach RCM, *Modelling pesticide leaching at a regional scale in the Netherlands*, National Institute of Public Health and the Environment, Report no 715801008, Bilthoven, The Netherlands (1996).
- Dikau R, *Experimentelle Untersuchungen zu Oberflächenabfluß und Bodenabtrag von Meßparzellen und landwirtschaftlichen Nutzflächen*, Geographisches Institut der Universität Heidelberg, Germany (1986).
- Knisel WG, *CREAMS: a field-scale model for chemicals, runoff and erosion from agricultural management systems*, USDA, Conservation Research Report 26 (1980).
- Hough MN, *Agrometeorological aspects of crops in the United Kingdom and Ireland. A review for sugar beet, oilseed rape, peas, wheat, barley, oats, potatoes, apples and pears*, Commission of the European Communities, EUR 13039 (1980).
- Perl, www.perl.com.
- Roulier S and Jarvis NJ, Modeling macropore flow effects on pesticide leaching: inverse parameter estimation using microlysimeters. *J Environ Qual* 32:2341–2353.
- Weiss R and Smith L, Efficient and responsible use of prior information in inverse methods. *Ground Water* 36:151–163 (1998).
- Carrera J and Neuman SP, Estimation of aquifer parameters under transient and steady state conditions: 2. Uniqueness, stability and solution algorithms. *Water Resour Res* 22:211–227 (1986).
- Dubus IG, Brown CD and Beulke S, Sources of uncertainty in pesticide fate modelling. *Sci Tot Environ* 317:53–72.
- Abbaspour KC, van Genuchten MT, Schulin R and Schlappi E, A sequential uncertainty domain inverse procedure for estimating subsurface flow and transport parameters. *Water Resour Res* 33:1879–1892 (1997).
- Gottesbüren B, Vormbrock N and Kallrath J, *Project SUSE: Sensitivity and uncertainty analysis of pesticide leaching models*, BASF AG internal report (1996).
- Dieses AE, Schlöder JP, Bock HG, Richter O, Aden K and Gottesbüren B, A parameter estimation tool for nonlinear transport and degradation processes of xenobiotics in soil,

- in *Human and environmental exposure to xenobiotics*, ed by Del Re AAM, Brown CD, Capri E, Errera G, Evans SP and Trevisan M, La Goliardica Pavese, Pavia, Italy, pp 171–180 (1999).
- 31 Heistermann M, Jene B, Fent G, Feyerabend M, Seppelt R, Richter O and Kubiak R, Modelling approaches to compare sorption and degradation of metsulfuron-methyl in laboratory micro-lysimeter and batch experiments. *Pest Manag Sci* **59**:1276–1990 (2003).
- 32 Toorman AF, Wierenga PJ and Hills RG, Parameter estimation of hydraulic properties from one-step outflow data. *Water Resour Res* **28**:3021–3028 (1992).